Fundamental Research 4 (2024) 882–889

Contents lists available at ScienceDirect

Fundamental Research

journal homepage: http://www.keaipublishing.com/en/journals/fundamental-research/

Article

# The siphonic energy transfer between hot solar wind and cold martian ionosphere through open magnetic flux rope

Xiaojun Xu[a,b,*], Lou-Chuang Lee[c], Qi Xu[d], Qing Chang[a,b], Jing Wang[e], Ming Wang[f], Shaosui Xu[g], Christian Möstl[h], Charles J. Farrugia[i], Xing Wang[a,b], Yudong Ye[a,b], Zilu Zhou[a,b], Lei Luo[a,b], Peishan He[a,b], Shaoguan Cheng[a,b]

[a] State Key Laboratory of Lunar and Planetary Sciences, Macau University of Science and Technology, Macau 999078, China
[b] CNSA Macau Center for Space Exploration and Science, Macau 999078, China
[c] Institute of Earth Science, Academia Sinica, Taipei 115029, China
[d] Institute of Space Science and Applied Technology, Harbin Institute of Technology, Shenzhen 518000, China
[e] Planetary Environmental and Astrobiological Research Laboratory (PEARL), School of Atmospheric Sciences, Sun Yat-sen University, Zhuhai 519000, China
[f] Nanjing University of Information Science and Technology, Nanjing 210000, China
[g] Space Science Laboratory, University of California, Berkeley CA 94320, USA
[h] Space Research Institute, Austrian Academy of Sciences, Graz 8010, Austria
[i] University of New Hampshire, NH 03824, USA

ARTICLE INFO

*Article history:*
Received 26 November 2021
Received in revised form 31 March 2022
Accepted 5 April 2022
Available online 28 April 2022

*Keywords:*
Mars
Flux rope
Solar wind
Ionosphere
Ion loss

ABSTRACT

A mechanism for energy transfer from the solar wind to the Martian ionosphere through open magnetic flux rope is proposed based on the observations by Mars Atmosphere and Volatile EvolutioN (MAVEN). The satellite was located in the dayside magnetosheath at an altitude of about 700 km above the northern hemisphere. Collisions between the hot solar wind protons and the cold heavy ions/neutrals in the subsolar region can cool the protons and heat the heavy ions. As a result, the magnetosheath protons are siphoned into the ionosphere due to the thermal pressure gradient of protons and the heated heavy ions escape along the open magnetic field lines. Although direct collisions in the lower-altitude region were not detected, this physical process is demonstrated by MAVEN measurements of enhanced proton density, decreased proton temperature and oppositely directed motions of hot and cool protons within the flux rope, which are very different from the observational features of the flux transfer events near the Earth's magnetopause. This mechanism could universally exist in many contexts where a collisionless plasma region is connected to a collisional plasma region. By reconstructing the magnetic geometry and the cross-section of the flux rope using the Grad-Shafranov technique, the ion loss rates are quantitatively estimated to be on the order of $10^{23}$ $s^{-1}$, which is much higher than previously estimated.

## 1. Introduction

The atmospheric loss to space is the most likely reason for the climate change in Mars. Many mechanisms have been proposed to interpret the atmospheric loss of Mars [1]. The solar wind provides part of the energy input that leads to the ion loss of Mars. However, the direct observations of particle energy transfer from the solar wind to the ionosphere of Mars have not been reported yet.

The solar wind interaction with Mars is the key to understand the atmospheric loss of Mars. Due to the lack of a global intrinsic magnetic field, the solar wind interacts directly with the highly conducting ionosphere. As a result of the super-magnetosonic solar wind, a bow shock forms upstream of the obstacle (Mars). Behind the bow shock is a magnetosheath with highly turbulent magnetic field and plasma. The interplanetary magnetic field (IMF) lines drape around Mars because of the deceleration of magnetic field lines near Mars due to massloading effect [2–6]. Because the weak plasma pressure of the Martian ionosphere cannot sustain the solar wind pressure, the IMF can usually enter into the ionosphere of Mars. Although the global magnetosphere has been lost, Mars has strong crustal magnetic fields nonuniformly distributed on the surface [7]. The topology of the magnetic field can be very complex. Using high-resolution electron spectra in the directions parallel and antiparallel to magnetic field, Xu et al. [8] developed so called "shape parameters" to indicate the different topologies of the magnetic field lines.

Flux ropes are also often detected during the interaction between the solar wind and the unmagnetized planet [9–11] or Mars with strong crustal fields [12–14]. Several mechanisms have been proposed to in-

* Corresponding author.
*E-mail address:* xjxu@must.edu.mo (X. Xu).

https://doi.org/10.1016/j.fmre.2022.04.014

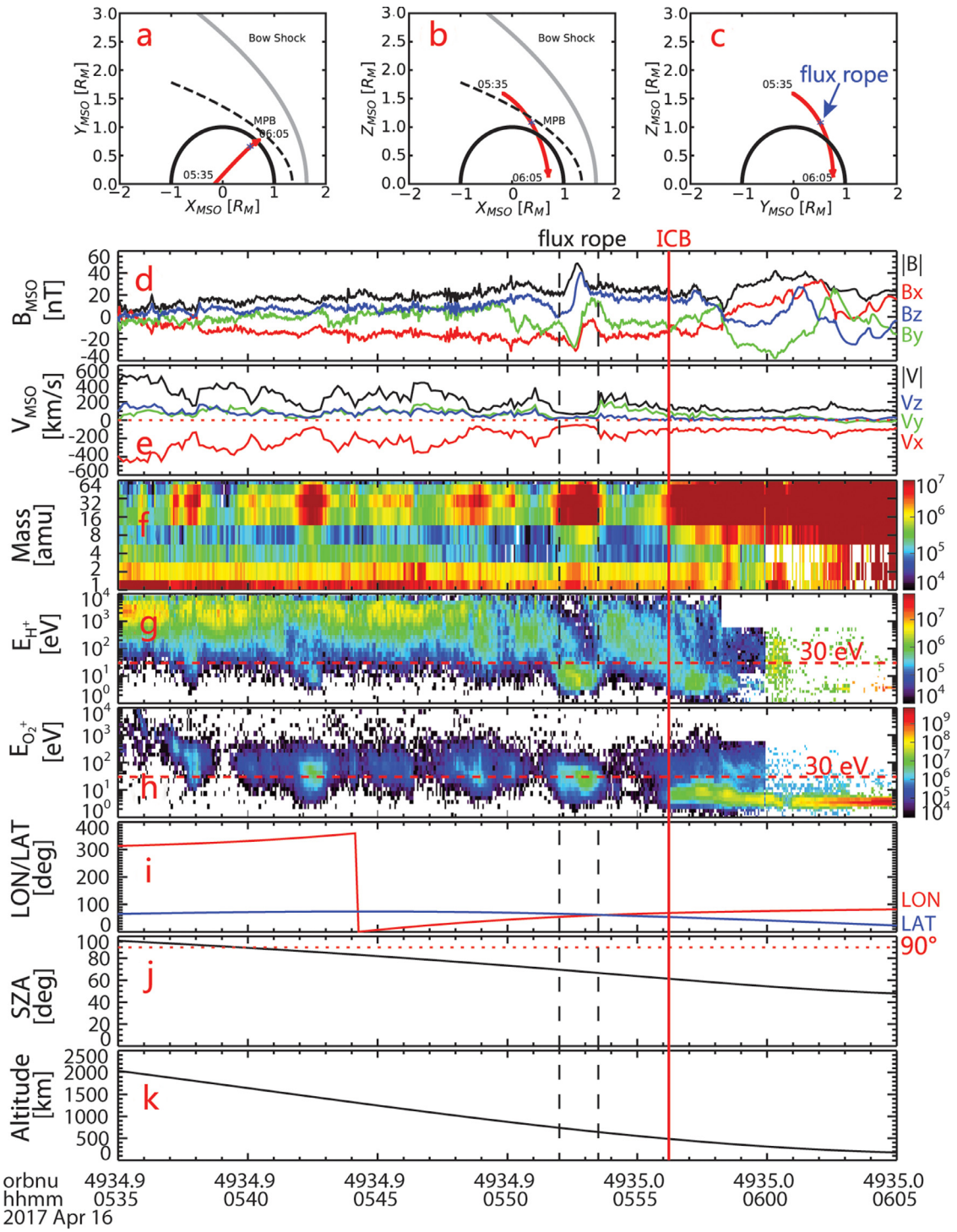


**Fig. 1. Selected magnetic field and plasma measurements and the positions of MAVEN when moving from magnetosheath to the ionosphere**. (a)–(c) MAVEN trajectory in the X-Y, X-Z, and Y-Z planes of the MSO coordinate system, respectively. (d) Magnetic field magnitude and the three components in MSO system. (e) Solar wind proton speed and velocity vector measured by SWIA in the MSO frame. (f) Mass spectrum measured by STATIC. (g) $H^+$ energy spectrum by STATIC. Most protons within the flux rope are below 30 eV. (h) $O_2^+$ energy spectrum from STATIC. The average energy is about 30 eV as indicated by the red dashed line. (i) The longitude and latitude profiles of MAVEN trajectory. (j) The solar zenith angle (SZA). (k) Altitude. The two vertical dashed lines mark the boundaries of the flux rope. The vertical red line marks the ICB.

terpret the formation of flux ropes [15]. Wolff et al. [16] suggested that Kelvin-Helmholtz instability (KHI) originating at the interface between the solar wind flow and ionosphere allows draped magnetic field lines become twisted in the ionosphere. Partially and fully developed vortices with twisted and enhanced magnetic fields have been reported [17,18]. Multiple X-line reconnection as proposed by Lee and Fu [19] is believed to account for the formation of most flux ropes near Earth [14,15,20–24], and many magnetic reconnection events have been identified in the Mars' space environment [25–29]. Dynamo generations of flux ropes have also been proposed by Luhmann and Elphic [30] as well as by Xie et al. [31] and Xie et al. [32] in recent studies. Brain et al. [33] reported that the dayside crustal fields are stretched tailward and may detach via

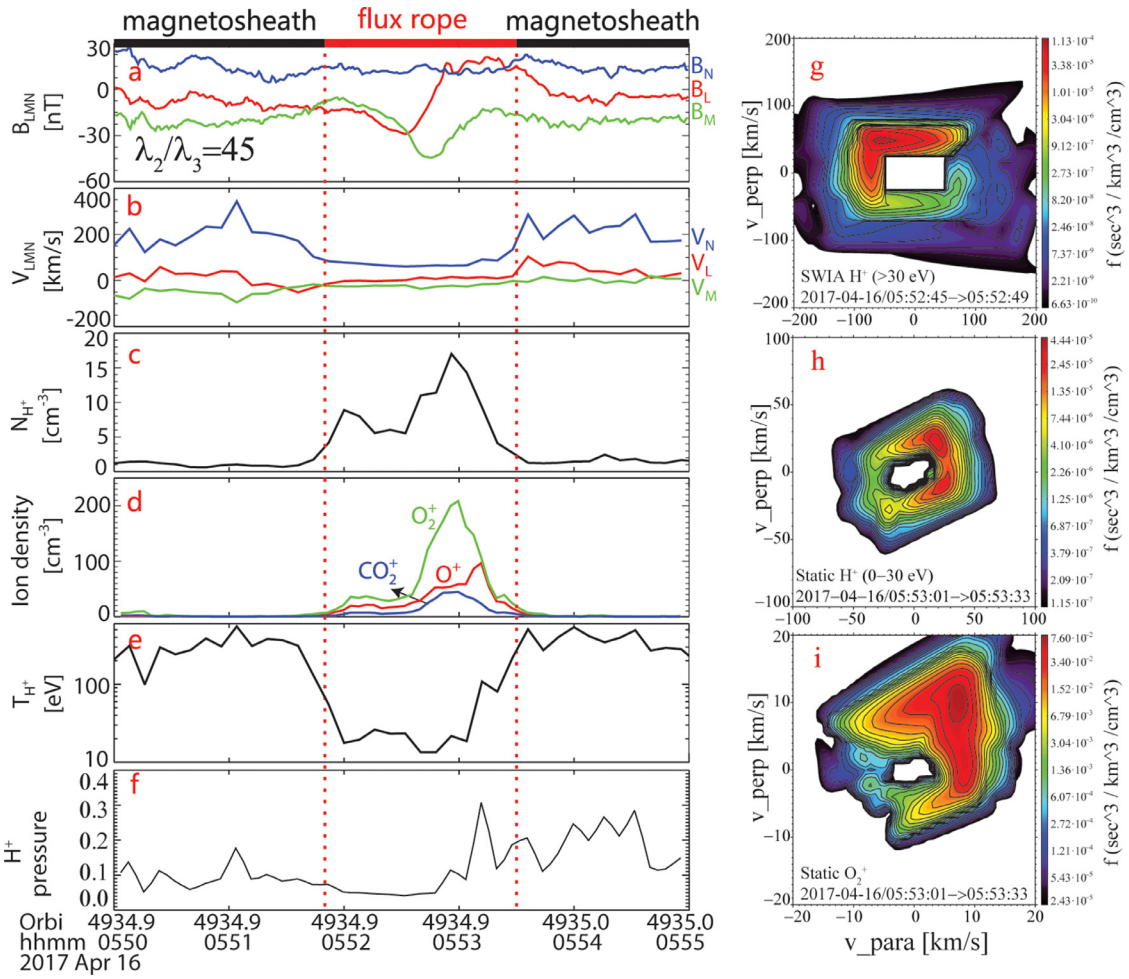


**Fig. 2. The LMN analysis of the magnetic field and selected plasma parameters calculated from STATIC around the flux rope.** (a) Magnetic vector in the LMN system. (b) The proton velocity in the LMN system. (c) Proton density. (d) Densities of heavy ions. (e) Proton temperature. (f) Proton thermal pressure. The vertical dashed lines mark the boundaries of the flux rope. (g)–(i) Parallel and perpendicular (to magnetic field) velocity distributions of $H^+$ with energies greater than 30 eV by SWIA, $H^+$ less than 30 eV by STATIC and $O_2^+$ by STATIC, respectively.

magnetic reconnection. Flux ropes are found to be capable of enhancing the ion loss of Mars [22,23]. It should be noted that different magnetic topologies could have significantly different influences on the ion loss rate of Mars [34].

In this study, we identified an open magnetic flux rope in the magnetosheath of Mars, reconstructed the geometry of the flux rope using Grad-Shafranov (GS) technique with single-spacecraft measurements [35], and quantitatively estimated the ion loss of the primary ions, $O_2^+$, $O^+$ and $CO_2^+$. Based on the observations, we suggest a mechanism for the energy transfer from the solar wind to ionosphere.

## 2. Data and instrumentation

The MAVEN spacecraft travels in an orbit of 150 km × 6200 km with an inclination angle of 75° and a period of 4.5 hr since being inserted into Mars' orbit in September 2014 [36]. MAVEN changes its orbit to 150 km 4500 km after May 2019. MAVEN consists of very comprehensive instruments measuring both field and particles to investigate the solar wind interaction with Mars as well as the relevant atmospheric loss. The Magnetometer (MAG) measures the three-component magnetic field at a cadence of 32 samples/s covering the range from 0.1 nT to 60,000 nT [37]. The Solar Wind Ion Analyzer (SWIA) measures the properties of solar wind and magnetosheath ions (mainly protons), providing the moment data of solar wind protons [38]. The Solar Wind Electron Analyzer (SWEA) can measure the energy and angular distributions of 3–4600 eV electrons [39]. The Suprathermal and Thermal Ion Composition (STATIC) analyzer [40] is designed to measure the ion mass compositions in the energy and angular distributions. STATIC provides the 3D ion (including proton) distributions with time resolutions of 4–128 s in the energy range of 0.1 eV–30 keV. It can produce 22 different data products, or Application Identifiers (APID). The STATIC APIDs of the C6 and D0 modes (32 energy channels, 64 mass bins, and time resolution of 128 s) are used. Note that SWIA data of proton could be sometimes contaminated by other species.

In the present study, we use data obtained from the four instruments above. The Mars-centered Solar Orbital (MSO) coordinate system is used unless indicated otherwise. The MSO coordinate system is defined with the X axis toward the Sun, the Z axis perpendicular to the ecliptic pointing to the northern hemisphere, and the Y axis completing the right-handed system.

## 3. MAVEN observations

During 05:35–06:05 UT on 16 April 2017, MAVEN moved from the dayside magnetosheath to the ionosphere of the Mars. Fig. 1 displays the selected measurements from MAVEN showing an overview of this event. The two vertical dashed lines mark the boundaries of the flux rope with enhanced magnetic strength and smoothly rotated magnetic direction. We can see that this flux rope was located in the magnetosheath. The magnetic field shown in Fig. 1d around the flux rope is

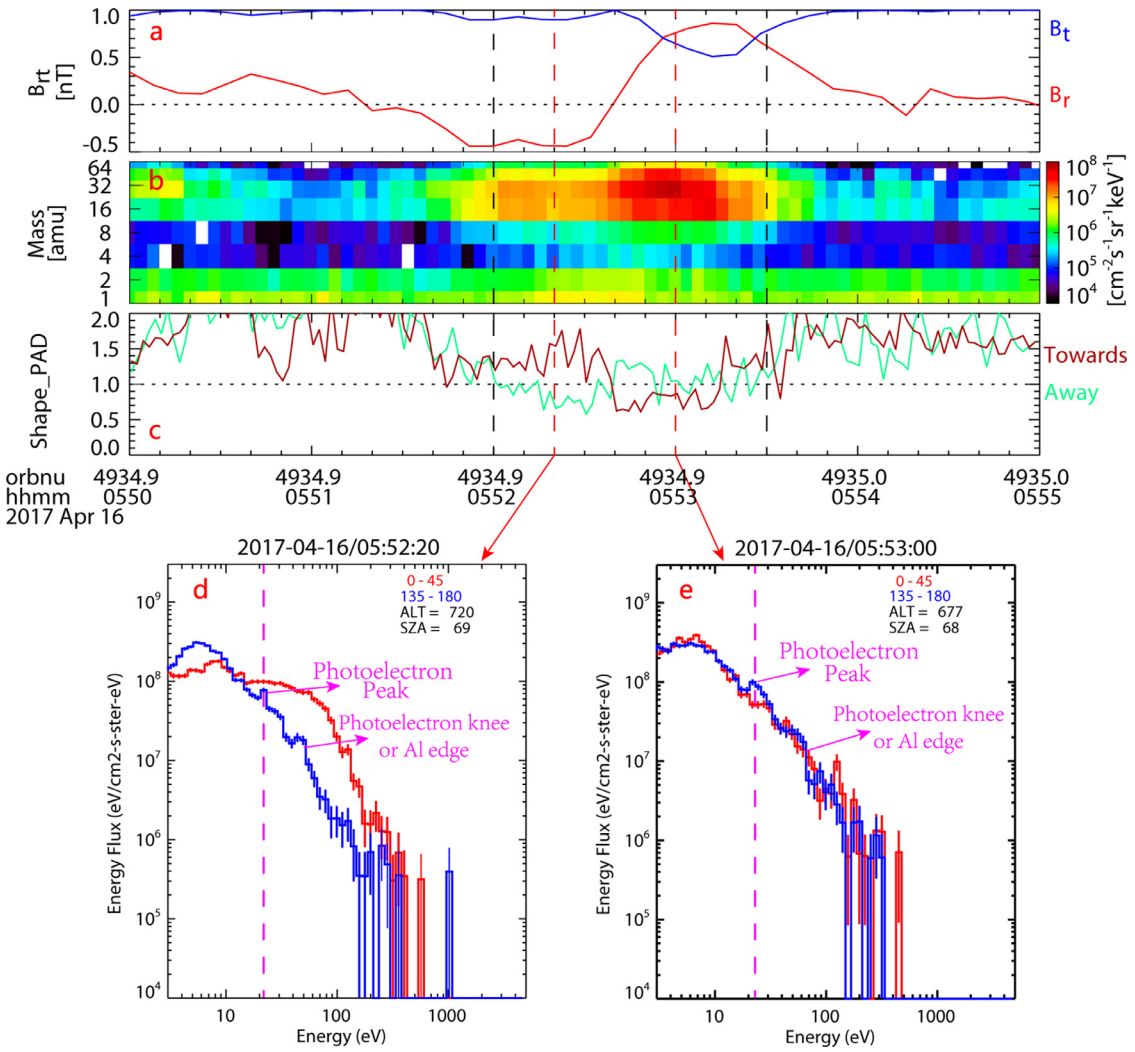


**Fig. 3. Analysis of the magnetic topology around the flux rope.** (a) The radial and tangential components of magnetic field. (b) The mass spectrum to indicate the boundaries of the flux rope. (c) The shape parameters. (d)–(e) Electron spectra at time slots as marked by the red arrows. The red curves represent the spectra of parallel electrons with pitch angles from 0 to 45° and the blue curves display the spectra of antiparallel electrons with pitch angles from 135° to 180°.

highly fluctuating. The fluxes of different ions presented in Fig. 1f– h also clearly indicate that the flux rope was well above the ion composition boundary (ICB), which is identified by the sharp drop of the heavy ion densities or fluxes. Fig. 1i–k show that the flux rope was detected on the dayside at an altitude of about 700 km over the northern hemisphere.

Fig. 1d shows that the magnetic strength is significantly enhanced within the flux rope and the magnetic field direction rotates smoothly across the flux rope. These are typical magnetic characteristics of flux ropes. Meanwhile, both the proton and heavy ion fluxes increased within the flux rope as presented in Fig. 1f–h, which indicates that the total pressure (sum of magnetic pressure and thermal pressure) is probably not balanced across the flux rope. Therefore, the magnetic tension due to bent magnetic field lines is required to balance the total pressure gradient. The magnetic topology of the flux rope can provide sufficient magnetic tension for balancing the stronger total pressure within the flux rope. The velocity of the proton shown in Fig. 1e is significantly lower within the flux rope with respect to the ambient sheath plasma. The energies of these proton are also lower than those of ambient protons (Fig. 1g), indicating that the sheath plasma within the flux rope has been significantly decelerated, while the heavy ions have been accelerated in comparison with those at the ICB near 05:59 UT, as displayed in Fig. 1h.

In order to investigate the features of the flux rope, we constructed the LMN coordinates using minimum variance analysis of magnetic field (MVAB) method [41] so that $\boldsymbol{L}$ is the field reversal direction, $\boldsymbol{N}$ is the normal (to the axis of the flux rope) direction and $\boldsymbol{N} \times \boldsymbol{L}$ forms $\boldsymbol{M}$. The $\boldsymbol{L}$, $\boldsymbol{M}$ and $\boldsymbol{N}$ by MVAB from 05:50 to 05:55 UT are derived to be [0.39, 0.53, 0.75], [0.37, 0.66, -0.66], [-0.85, 0.53, 0.06] in MSO coordinates, respectively. Fig. 2 shows selected parameters in the LMN coordinate system. The ratio of the intermediate eigenvalue to the minimal eigenvalue is 45. The three magnetic field components (Fig. 2a) are consistent with the flux rope configuration: a smooth rotation of the magnetic direction and significant enhancements of magnetic strength in the axial direction ($\boldsymbol{M}$). However, the absence of bipolar structures in the $\boldsymbol{B}_{\boldsymbol{N}}$ component strongly suggests that the flux rope was not produced by magnetic reconnection in current sheet. Fig. 2b shows that there is almost no acceleration in the $\boldsymbol{L}$ direction, which is not in agreement with reconnection. In addition, the proton temperature (Fig. 2e) greatly decreased from about 400 to 20 eV, which is also not consistent with reconnection. Fig. 2c and d clearly show greatly enhanced sheath protons and heavy ions within the flux rope. The proton and heavy ions, especially $O_2^+$, have very similar density profiles, indicating they are fully mixed. It is important to point out that the density of protons increased rather than decreased as in the flux transfer events observed near Earth, in which plasma is squeezed out [42]. However, the proton thermal

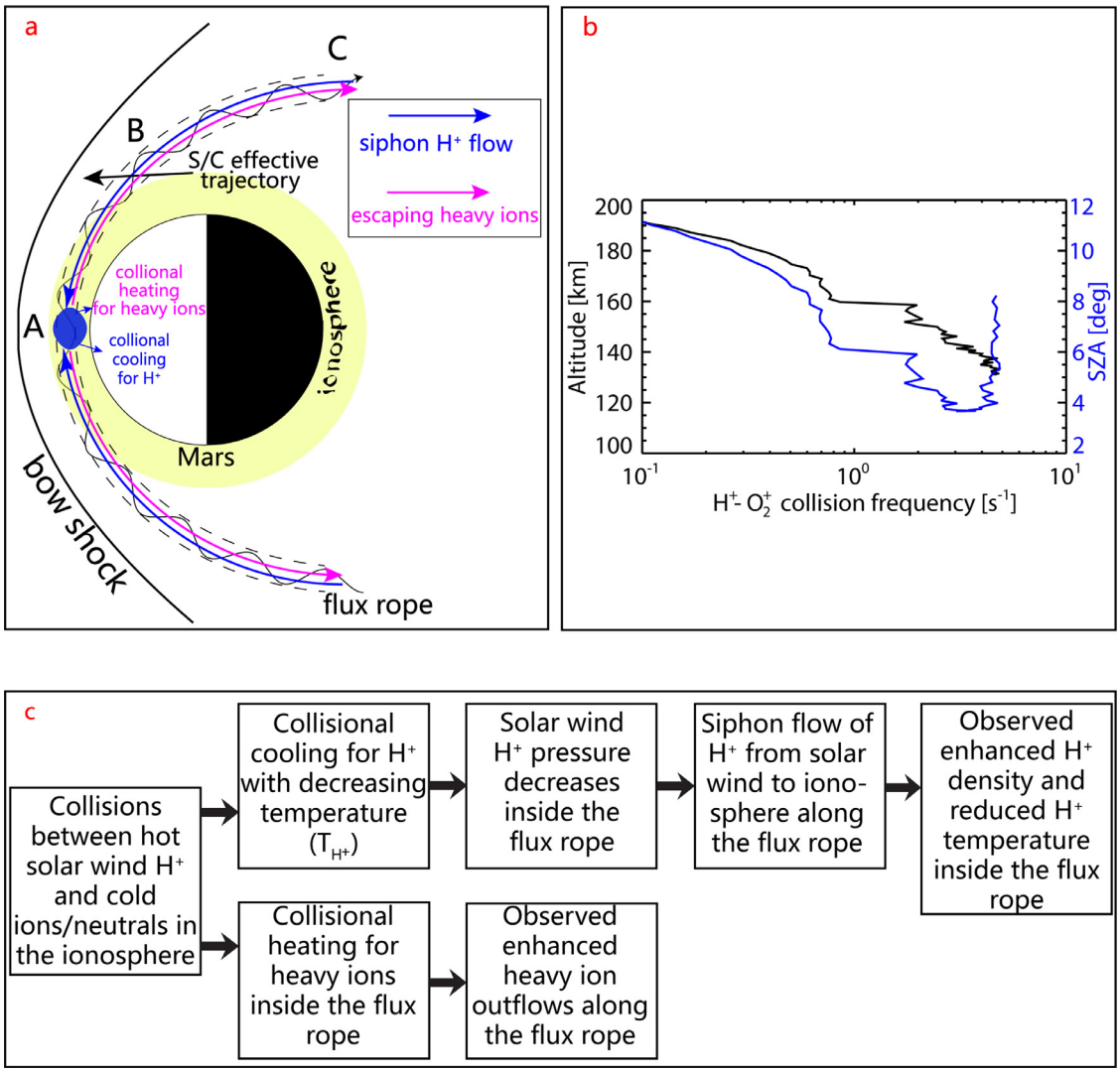


**Fig. 4. Illustration and diagram of the mechanism for energy transfer from solar wind to Martian ionosphere (not to scale).** (a) The sketch of the energy transfer by collisions between the solar wind protons and ionospheric ions through open flux rope. Through collisions, the solar wind energy is transferred to the Martian ionosphere. As a result, the proton temperature as well as the thermal pressure decrease greatly. The hot sheath protons are thus siphoned into the region where collisions take place. The cooled protons together with the heated heavy ions can escape through the open flux rope and be picked up by the solar wind. (b) The collision frequency, which indicates the time scale of collision between $H^+$ and $O_2^+$. (c) The diagram to interpret how the collisions between hot solar wind $H^+$ and cold ions or neutrals to siphon the solar wind $H^+$ and heat the heavy ions to escape.

pressure within the flux rope was still lower than that of the ambient sheath plasma. Fig. 2g–i present the velocity distributions of hot protons (≥ 30 eV), cool protons (0–30 eV) and $O_2^+$, respectively. Considering that the $\boldsymbol{M}$ direction as shown above is in the $-Z_{MSO}$ direction and the core magnetic field has a major $-B_M$ component, we can verify that the magnetic field direction is in the $+Z_{MSO}$. Since MAVEN was located above the northern hemisphere, the mainly $-V_{\parallel}$ of hot protons demonstrated they were moving inwards to the subsolar region, while the cool protons and $O_2^+$ were similarly moving outwards.

If the flux rope is topologically open with magnetic field lines connecting the solar wind and ionosphere, ion loss could be continuing due to the pressure gradient [34] until the flux rope detaches from the ionosphere of Mars. Using the electron measurements by MAVEN/SWEA, we obtained the shape parameter with values well above 1 indicating the solar wind electrons and well below 1 indicating the ionospheric electrons [8]. Fig. 3 shows the magnetic topology analysis of this flux rope. Fig. 3a presents the radial and tangential magnetic components. Because of the magnetic field direction rotation, the radial component ($B_r$) changed from negative (pointing to Mars) to positive (pointing to space) at ~05:52:40 UT. Fig. 3b re-plots the mass spectrum to show the boundaries of the flux rope. The shape parameters are displayed in Fig. 3c. It can be easily seen that the two shape parameters have one above 1 and the other below 1 at most places of the flux rope, which indicates that the magnetic fields of the flux rope are open [8]. We selected two time slots within the flux rope, 05:52:20 and 05:53:00 UT, to show the electron spectra in the parallel and antiparallel directions. As illustrated in Fig. 3d and 3e, obvious photoelectron peaks (~ 23 eV) exist in the antiparallel direction electron spectrum. The photoelectron knee [8] or Al edge [43] at ~60 eV, another characteristic of ionospheric electron spectrum, also appears in the antiparallel direction. But the parallel spectrum shows no features of ionospheric electrons. Although, the parameters being near 1 bring some ambiguity, these two electron spectra roughly reveal that the flux rope is topologically open with one foot in the ionosphere and the other in the solar wind.

Here, we suggest a mechanism to interpret the observations of this event. As illustrated in Fig. 4a, the diagram in Fig. 4c shows how collisions occurring in the subsolar region of the ionosphere transfer the energy from the hot solar wind $H^+$ to ionospheric particles. It should be

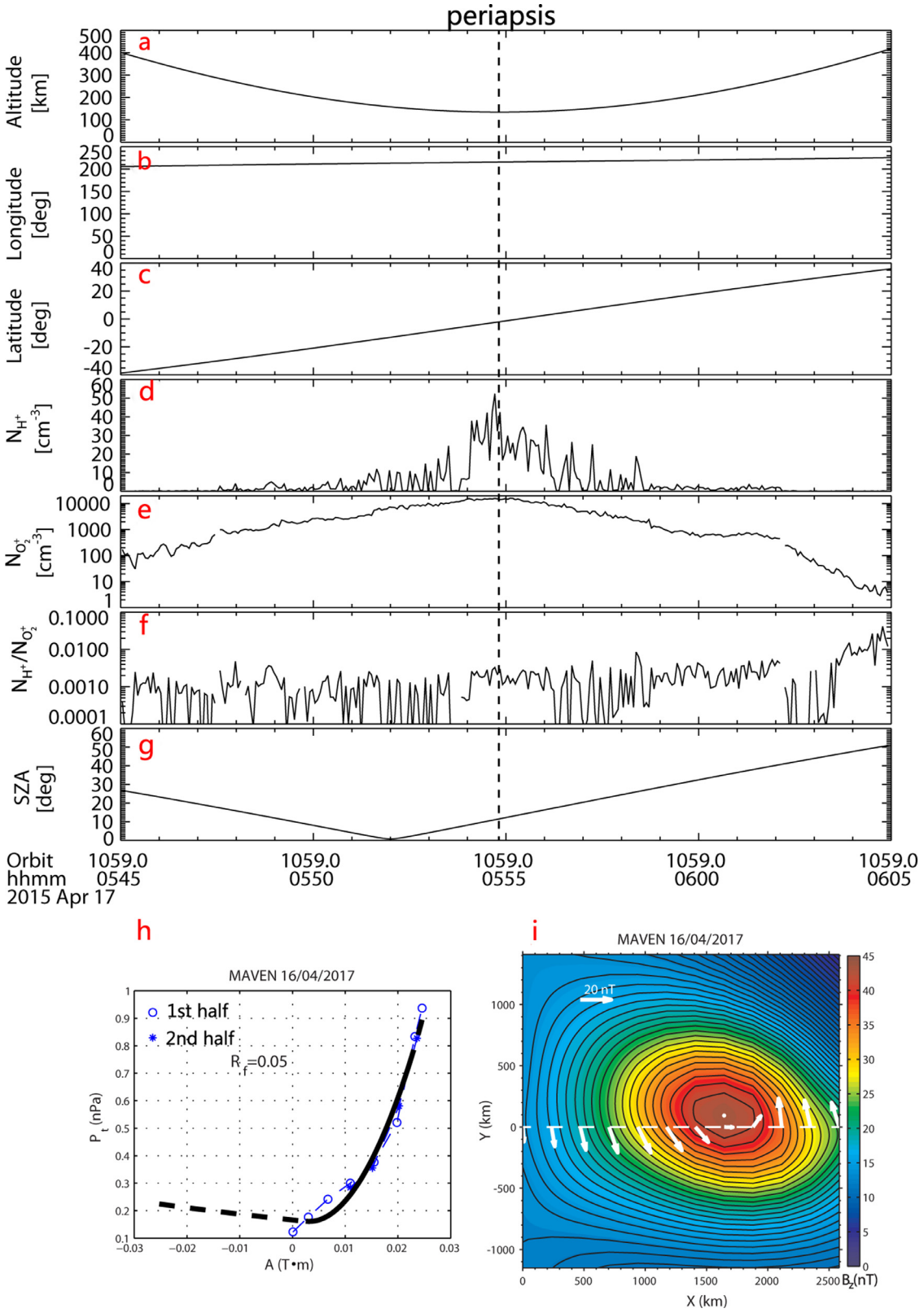


**Fig. 5. Selected parameters by MAVEN and the flux rope geometry reconstructed by the GS reconstruction technique in the deHoffmann-Teller frame, in which there should be no electric field and thus the magnetic field is steady** ($\nabla \times \boldsymbol{E} = -\partial \boldsymbol{B}/\partial t = 0$)**.** (a)–(g) Altitude, longitude, latitude, proton density, $O_2^+$ density, $n_{H^+}/n_{O_2^+}$, and SZA, respectively. (h) The data plot and fitting curve of $P_t(A)$. (i) Reconstructed geometry of the flux rope. The black solid lines represent the magnetic field lines with white arrows indicating the magnetic field directions and the lengths of arrows indicating the magnetic magnitude. The axial magnetic strength of the flux rope is shown by the color scale.

pointed out that the wave-particle interaction driven by the downward solar wind protons can also transfer the solar wind energy into the ionosphere [44]. However, the direct collisions should be much more efficient in energy transfer than wave-particle interaction. Fig. 4b shows the collision frequency, $\nu_{H^+O_2^+} = 1.25 n_{O_2^+}/T_{O_2^+}^{3/2}$ [45], using the density and temperature of $O_2^+$ from MAVEN measurements during the "deep dip" from 17 April 2015 to 22 April 2015 to altitudes just below 130 km with low solar zenith angles less than 15°. We can see that the timescale of collision can be less than 1 s, while the timescale for the flux rope staying in the subsolar ionosphere should be much greater than the time interval of MAVEN crossing the flux rope in the magnetosheath (~1 min). The thermal and sonic speeds of the sheath $H^+$ derived by the average temperature in the ambient sheath (about 400 eV) are 277 km/s and 253 km/s, respectively. The timescale for the hot sheath $H^+$ refilling into the subsolar region through the open flux rope is about 10 s, i.e., a distance of $\pi/4 * R_M$, where $R_M$ is Mars' radius, via the refilling speed being the sound speed. Therefore, the collision and refilling processes are rapid enough to transfer the energy from the solar wind to the ionosphere through the open flux rope.

It should be pointed out that a portion of cold protons could be originally from the ionosphere. However, the density ratio ($n_{H^+}/n_{O_2^+}$) is around 0.1, much higher than that (~0.001) in the ionosphere model of Mars [46] and those measured by during MAVEN during the "deep dip". Fig. 5a–h show selected parameters near the periapsis of Orbit 1059 on 17 April 2015. The $n_{H^+}/n_{O_2^+}$ with relatively high $n_{H^+}$ stays around 0.001 in the subsolar region and shows no difference in the southern hemisphere with strong crustal magnetic fields. Such high values of $n_{H^+}/n_{O_2^+}$ indicate that not all the protons are originally from the ionosphere.

The GS technique can reconstruct the magnetic geometry in a plane perpendicular to the axis and obtain the size of the flux rope. Fig. 5h and i displays the result of the GS reconstruction. The axis direction is calculated to be [-0.63, -0.29, 0.72] in MSO coordinates. The reconstruction is valid for a magnetostatic structure with an invariant direction (i.e., an axis). From Fig. 5, we can roughly treat the flux rope as an ellipse with a semi-major axis of 1000 km along the horizonal direction and a semi-minor axis of 750 km along the vertical direction. The ion loss rate can be calculated by $R = \bar{n} v S$, where $\bar{n}$ is the average density, $v$ is the ion speed and $S$ is the cross-section of the flux rope. Here, the velocities of the heavy ions aligned to the axis of the flux rope are used, 8.17, 7.76, 7.11 km/s for $O_2^+$, $O^+$, $CO_2^+$, respectively. $\bar{n}$ are 73.40, 33.93, 15.83 $cm^{-3}$ for $O_2^+$, $O^+$, $CO_2^+$, respectively. Therefore, the loss rates are $3.35 \times 10^{23}$ $s^{-1}$ for $O_2^+$, $1.63 \times 10^{23}$ $s^{-1}$ for $O^+$, $0.67 \times 10^{23}$ $s^{-1}$ for $CO_2^+$. These ion loss rates are one order higher than previously estimated by Hara et al. [22].

## 4. Discussions and Conclusion

In this paper, we identified a flux rope in the magnetosheath of Mars, which was placed at an altitude of 700 km in the dayside over the northern hemisphere. The heavy ion fluxes with energies greater than the escape energy are greatly enhanced within the flux rope. This open magnetic flux rope could provide a channel that leads to continuous ion loss from Mars. We quantitatively estimated the ion loss rate of the three main heavy ions of the Martian ionosphere: $O_2^+$, $O^+$, $CO_2^+$, and found that the total ion loss rate is $5.65 \times 10^{23}$ $s^{-1}$ and the total oxygen loss rate is about $9.67 \times 10^{23}$ $s^{-1}$. This loss rate reaches ~60% of the total ion escape estimated by Mars Express [~ $10^{24}$ $s^{-1}$; 47,48], or 16% of the total oxygen ion loss estimated by MAVEN [$6 \times 10^{25}$ $s^{-1}$; 1].

The flux rope in this study is very different from typical FTEs near Earth with enhanced densities and temperatures. To interpret these two different features, we suggest a mechanism of collisions between hot solar wind protons and cold ionospheric ions in the lower ionosphere. Through collisions, the solar wind energy is transferred to the Martian ionosphere. As a result, the proton temperature as well as the thermal pressure decrease greatly. The hot sheath protons are thus siphoned into the region where collisions take place. The cooled protons together with the heated heavy ions can escape through the open flux rope and be picked up by the solar wind. MAVEN crossed the intermediate part of the flux rope between the collision region and the outer sheath, and observed the bidirectional motions or a mixture of the hot protons and cold protons. Therefore, the proton density and temperature should be between those in the collision region and the ambient sheath. Note that, although the total thermal pressure in the collision region increases, the outer hot protons can be still siphoned inwards. The reason is that the protons have much higher thermal or sonic speed than heavy ions. They cannot feel the thermal pressure of other ions in the collisionless regime. That is why different compositions have different scale heights in the upper ionosphere.

It is important to be pointed out that this mechanism does not require the presence of flux ropes. It can also work through open magnetic field lines. However, the flux rope, having a strong boundary, can better confine the motions of different ions. If the open field lines in the sheath (in the Place C of Fig. 4a) extend widely, the proton density probably cannot show enhancement, but the depletion of proton temperature should be still noticed. This mechanism probably widely exists in the contexts where a collisionless plasma region is connected to a collisional plasma region and plays an important role in the energy transfer from solar wind to unmagnetized planetary ionosphere that can lead to atmospheric loss.

## Declaration of competing interest

The authors declare that they have no conflicts of interest in this work.

## Acknowledgments

This work is funded by National Natural Science Foundation of China (42122061), the Science and Technology Development Fund of Macao SAR (0002/2019/A1), Macau Foundation, and the pre-research project on Civil Aerospace Technologies No. D020308 and D020104 funded by China National Space Administration. C.M. thanks the Austrian Science Fund (FWF): P31521-N27. C.J.F. thanks NASA grant: 80NSSC19K1293. A basic version of the Grad-Shafranov reconstruction method in Matlab is available at https://github.com/cmoestl/interplanetary-grad-shafranov. We acknowledge the MAVEN contract for support. All MAVEN data are available on the Planetary Data System (https://pds.nasa.gov).

## References

[1] B.M. Jakosky, D. Brain, M. Chaffin, et al, Loss of the martian atmosphere to space: Present-day loss rates determined from MAVEN observations and integrated loss through time, Icarus 315 (2018) 146–157.
[2] H. Alfven, On the theory of comet tails, Tellus 9 (1957) 92.
[3] C. Bertucci, F. Duru, N. Edberg, et al, The induced magnetospheres of mars, venus, and titan, Space Sci. Rev. 162 (1–4) (2011) 113–171.
[4] Q. Chang, X. Xu, T. Zhang, et al, Magnetic field near venus: Comparison between solar cycle 24 and previous cycles, Astrophys. J. 867 (2) (2018) 129.
[5] Q. Xu, X. Xu, Q. Chang, et al, Observations of the venus dramatic response to an extremely strong interplanetary coronal mass ejection, Astrophys. J. 876 (1) (2019) 84.
[6] J. Wang, L.C. Lee, X. Xu, et al., Plasma and magnetic-field structures near the martian induced magnetosphere boundary. i. plasma depletion region and tangential discontinuity, Astron. Astrophys. 642 (2020) A34.
[7] M.H. Acuna, J.E.P. Connerney, P. Wasilewski, et al., Magnetic field and plasma observations at mars: Initial results of, Science 279 (1998) 1676.
[8] S. Xu, D. Mitchell, M. Liemohn, et al., Martian low-altitude magnetic topology deduced from MAVEN/SWEA observations, J. Geophys. Res. Space Phys. 122 (2) (2017) 1831–1852.
[9] C.T. Russell, R.C. Elphic, Observation of magnetic flux ropes in the venus ionosphere, Nature 279 (5714) (1979) 616–618.
[10] R.C. Elphic, C.T. Russell, Magnetic flux ropes in the venus ionosphere: Observations and models, J. Geophys. Res. 88 (A1) (1983) 58–72.
[11] T.L. Zhang, W. Baumjohann, W.L. Teh, et al., Giant flux ropes observed in the magnetized ionosphere at venus, Geophys. Res. Lett. 39 (23) (2012) L23103.
[12] P.A. Cloutier, C.C. Law, D.H. Crider, et al., Venus-like interaction of the solar wind with mars, Geophys. Res. Lett. 26 (17) (1999) 2685–2688.

[13] D. Vignes, M.H. Acuña, J.E.P. Connerney, et al., Magnetic flux ropes in the martian atmosphere: Global characteristics, Space Sci. Rev. 111 (1) (2004) 223–231.
[14] T. Hara, K. Seki, H. Hasegawa, et al., The spatial structure of Martian magnetic flux ropes recovered by the Grad-Shafranov reconstruction technique, J. Geophys. Res. Space Phys. 119 (2) (2014) 1262–1271.
[15] C.F. Bowers, J.A. Slavin, G.A. DiBraccio, et al., MAVEN survey of magnetic flux rope properties in the Martian ionosphere: Comparison with three types of formation mechanisms, Geophys. Res. Lett. 48 (10) (2021) e93296.
[16] R.S. Wolff, B.E. Goldstein, C.M. Yeates, The onset and development of Kelvin-Helmholtz instability at the Venus ionopause, J. Geophys. Res. 85 (1980) 7697–7707.
[17] S. Ruhunusiri, J.S. Halekas, J.P. McFadden, et al., MAVEN observations of partially developed Kelvin-Helmholtz vortices at Mars, Geophys. Res. Lett. 43 (10) (2016) 4763–4773.
[18] G. Poh, J.R. Espley, K. Nykyri, et al., On the growth and development of non-Linear kelvin-Helmholtz instability at mars: MAVEN observations, J. Geophys. Res. Space Phys. 126 (9) (2021) e29224.
[19] L.C. Lee, Z.F. Fu, A theory of magnetic flux transfer at the Earth's magnetopause, Geophys. Res. Lett. 12 (2) (1985) 105–108.
[20] M.J. Beharrell, J.A. Wild, Stationary flux ropes at the southern terminator of mars, J. Geophys. Res. Space Phys. 117 (2012) A12212.
[21] T. Hara, K. Seki, H. Hasegawa, et al., Formation processes of flux ropes downstream from Martian crustal magnetic fields inferred from grad-Shafranov reconstruction, J. Geophys. Res. Space Phys. 119 (9) (2014) 7947–7962.
[22] T. Hara, D.L. Mitchell, J.P. McFadden, et al., Estimation of the spatial structure of a detached magnetic flux rope at Mars based on simultaneous MAVEN plasma and magnetic field observations, Geophys. Res. Lett. 42 (21) (2015) 8933–8941.
[23] T. Hara, D.A. Brain, D.L. Mitchell, et al., MAVEN Observations of a giant ionospheric flux rope near Mars resulting from interaction between the crustal and interplanetary draped magnetic fields, J. Geophys. Res. Space Phys. 122 (1) (2017) 828–842.
[24] T. Hara, Y. Harada, D.L. Mitchell, et al., On the origins of magnetic flux ropes in near–Mars magnetotail current sheets, Geophys. Res. Lett. 44 (15) (2017) 7653–7662.
[25] J.S. Halekas, J.P. Eastwood, D.A. Brain, et al., In situ observations of reconnection Hall magnetic fields at Mars: Evidence for ion diffusion region encounters, J. Geophys. Res. Space Phys. 114 (A11) (2009) A11204.
[26] Y. Harada, J.S. Halekas, J.P. McFadden, et al., Magnetic reconnection in the near-Mars magnetotail: MAVEN observations, Geophys. Res. Lett. 42 (21) (2015) 8838–8845.
[27] Y. Harada, J.S. Halekas, J.P. McFadden, et al., Survey of magnetic reconnection signatures in the Martian magnetotail with MAVEN, J. Geophys. Res. Space Phys. 122 (5) (2017) 5114–5131.
[28] Y. Harada, J.S. Halekas, G.A. DiBraccio, et al., Magnetic reconnection on dayside crustal magnetic fields at mars: MAVEN observations, Geophys. Res. Lett. 45 (10) (2018) 4550–4558.
[29] J. Wang, J. Yu, X. Xu, et al., MAVEN Observations of magnetic reconnection at martian induced magnetopause, Geophys. Res. Lett. 48 (21) (2021) A34.
[30] J.G. Luhmann, R.C. Elphic, On the dynamo generation of flux ropes in the Venus ionosphere, J. Geophys. Res. 90 (A12) (1985) 12047–12056.
[31] L. Xie, L.-C. Lee, A new mechanism for the field line twisting in the ionospheric magnetic flux rope, J. Geophys. Res. Space Phys. 124 (5) (2019) 3266–3275.
[32] L. Xie, L.-C. Lee, L. Li, et al., Multifluid MHD studies of the ionospheric magnetic flux ropes at mars, Astrophys. J. 915 (1) (2021) 6.
[33] D.A. Brain, A.H. Baker, J. Briggs, et al., Episodic detachment of Martian crustal magnetic fields leading to bulk atmospheric plasma escape, Geophys. Res. Lett. 37 (14) (2010) L14108.
[34] R.E. Ergun, L.A. Andersson, C.M. Fowler, et al., Enhanced $o_2^+$ loss at mars due to an ambipolar electric field from electron heating, J. Geophys. Res. Space Phys. 121 (5) (2016) 4668–4678.
[35] Q. Hu, B.U.Ö. Sonnerup, Reconstruction of magnetic clouds in the solar wind: Orientations and configurations, J. Geophys. Res. Space Phys. 107 (A7) (2002) 1142.
[36] B.M. Jakosky, R.P. Lin, J.M. Grebowsky, et al., The mars atmosphere and volatile evolution (MAVEN) mission, Space Sci. Rev. 195 (1–4) (2015) 3–48.
[37] J.E.P. Connerney, J. Espley, P. Lawton, et al., The MAVEN magnetic field investigation, Space Sci. Rev. 195 (1–4) (2015) 257–291.
[38] J.S. Halekas, E.R. Taylor, G. Dalton, et al., The solar wind ion analyzer for MAVEN, Space Sci. Rev. 195 (1–4) (2015) 125–151.
[39] D.L. Mitchell, C. Mazelle, J.A. Sauvaud, et al., The MAVEN solar wind electron analyzer, Space Sci. Rev. 200 (1–4) (2016) 495–528.
[40] J.P. McFadden, O. Kortmann, D. Curtis, et al., MAVEN Suprathermal and thermal ion compostion (STATIC) instrument, Space Sci. Rev. 195 (1–4) (2015) 199–256.
[41] B.U.O. Sonnerup, J. Cahill L. J., Magnetopause structure and attitude from explorer 12 observations, J. Geophys. Res. 72 (1967) 171.
[42] Z.W. Ma, A. Otto, L.C. Lee, Core magnetic field enhancement in single X line, multiple X line and patchy reconnection, J. Geophys. Res. 99 (A4) (1994) 6125–6136.
[43] G. Collinson, D. Mitchell, A. Glocer, et al., Electric Mars: The first direct measurement of an upper limit for the Martian "polar wind" electric potential, Geophys. Res. Lett. 42 (21) (2015) 9128–9134.
[44] C. Zhang, Z. Rong, H. Nilsson, et al., MAVEN observations of periodic low-altitude plasma clouds at mars, Astrophys. J. Lett. 922 (2) (2021) L33.
[45] R. Schunk, A. Nagy, Ionospheres: Physics, plasma physics, and chemistry, Cambridge university press, 2009.
[46] S.W. Bougher, D.A. Brain, J.L. Fox, et al., Upper Neutral Atmosphere and Ionosphere, 2017, pp. 405–432.
[47] S. Barabash, A. Fedorov, R. Lundin, et al., Martian atmospheric erosion rates, Science 315 (5811) (2007) 501.
[48] H. Nilsson, E. Carlsson, D.A. Brain, et al., Ion escape from Mars as a function of solar wind conditions: A statistical study, Icarus 206 (1) (2010) 40–49.

**Xiaojun Xu** (BRID: 08508.00.03079) is an associate professor at the State Key Laboratory of Lunar and Planetary Sciences (SKLplanets), Macau University of Science and Technology and the leader of Planetary Space Physics Group of SKLplanets. He received his Ph.D. degree from the National Space Science Center, Chinese Academy of Sciences. His research interests mainly focus on the solar wind and its interactions with the Moon and terrestrial planets.